4-D SEISMICS, GAS-HYDRATE DETECTION AND OVERPRESSURE PREDICTION AS A COMBINED METHODOLOGY FOR APPLICATION TO CO_2 SEQUESTRATION

Combined seismic methods for CO_2 monitoring

S. Persoglia, J.M. Carcione, G. Rossi And D. Gei
Istituto Nazionale di Oceanografia e di Geofisica – OGS-, Trieste, Italy

Abstract: Seismic surveys have proven to be useful for monitoring injected CO_2 in the subsurface. In this work, we show how rock physics, poro-elastic modeling and 3D seismic tomography can be combined to detect the subtle changes in seismic properties related to changes in pore-fill. 3D seismic tomography yields the P- and S-wave velocity cubes, which are converted to petro-physical properties by using rock-physics models of partial saturation under varying temperature and pressure conditions, and seismic numerical modeling. The methodology is illustrated with field examples of time-lapse analysis and gas-hydrate detection.

Key words: Seismic properties, tomography, poro-elasticity.

1. INTRODUCTION

The underground storage of CO_2 involves technologies developed and widely used by the oil and gas industries for exploration, exploitation and monitoring of hydrocarbon reservoirs. In CO_2 sequestration, the type of monitoring, its duration and frequency are key elements to verify the storage efficiency and distribution of the injected carbon dioxide. Seismic surveys have proven to be capable of monitoring CO_2 in the subsurface (e.g. Arts et al., 2004; Ghaderi and Landrø, 2004). To guarantee a similar success in less favourable geological contexts, it is therefore important to apply the most advanced methodologies to the specific case of CO_2 monitoring. In

S. Lombardi et al. (eds.),
Advances in the Geological Storage of Carbon Dioxide, 315–323.

particular, the combination of 3D seismic tomography and poro-elastic seismic modeling are powerful tools to tackle the injection problem.

In this work, we show field examples of time-lapse analysis, free-gas and gas-hydrate evaluation, and the detection of overpressure conditions in an effort to extend these techniques to CO_2 detection and monitoring.

2. SEISMIC TOMOGRAPHY

Time-lapse analysis, required to detect small changes in the reservoir due to fluid movements, often has the problem that the seismic data has been collected with different acquisition configurations and technologies, and thus special processing aimed at rendering the different data sets equivalent is required (e.g. Magesan et al., 2005). Another problem that may mask the velocity variations in the reservoir are the seasonal changes of the overburden (the sea-water layer in marine surveys or the water table on-land). The use of 3D time-lapse tomography has proven to be a flexible and powerful tool in solving both problems, enabling the removal of the related small velocity variations and giving a set of coupled models to highlight the reservoir changes (Vesnaver et al., 2003).

The tomographic inversion consists of minimizing the differences between the observed and calculated travel times, thus allowing to obtain the wave velocities. The travel time of seismic waves recorded by a geophone is obtained by integrating the slownesses along the ray path. The integral is replaced by a summation over the voxels, since a discrete blocky model is usually adopted. The travel time difference can be expressed as

$$\Delta t = t^{OBS} - t^{CALC} = \sum_j \Delta s_j \Delta u_j \ . \qquad 1$$

In practice, the tomographic inversion follows the scheme of Figure 1. The rays are first traced on an initial model, using the same acquisition geometry of the real experiment, and the obtained travel times are subtracted from those of the real experiment. The residuals are minimized to upgrade the velocity and geometrical features of the reflecting/refracting interfaces, until the model does not change compared to the previous one. The separate inversion of the velocity and interface depths and geometry makes the procedure less sensitive to cross talk between velocity and depth errors (Bishop et al., 1985; Bickel, 1990; Delprat-Jannaud and Lailly, 1992; Docherty, 1992; Lines, 1993; Tieman, 1994). The non-uniqueness of the solution is reduced by finding the optimal grid for the velocity field via adaptive irregular or staggered grids (e.g. Vesnaver and Böhm, 2000).

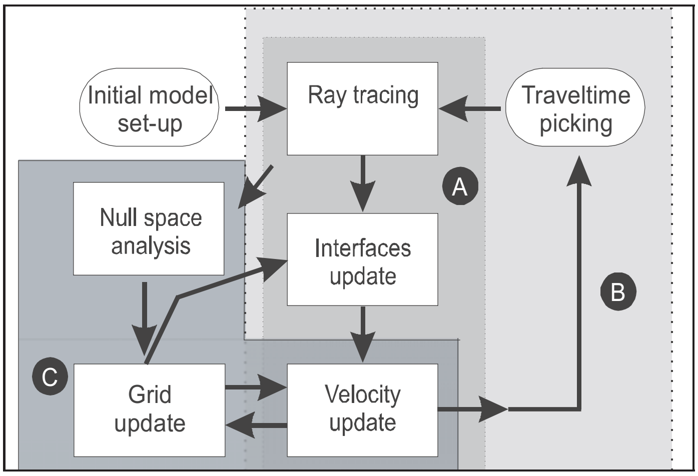

Figure 1. Scheme of the three main loops of the tomographic inversion. A) Update of the velocity field and interface depth; B) Picking and comparison with travel times from the tomographic model; C) Grid upgrading, based on velocity field and reliability.

The final result of the seismic tomography is therefore a velocity model in depth, where the geologic complexities are preserved. This output can be an optimal input for pre-stack depth migration to obtain an accurate imaging of the various geological features.

In the case of time-lapse analysis we can impose the additional constraint that the geometry and velocity of most of the model does not change over time, while leaving free the reservoir and the shallowest layer (which may be affected by seasonal variations). This procedure constitutes the basis of "Time-lapse tomography", successfully applied to different vintages acquired offshore Norway (Vesnaver et al., 2003). The data was acquired in 1989, with a single vessel towing two streamers and a central air gun, and in 1992, using one vessel with three streamers and a sleeve gun as source while a second vessel towed two additional streamers. In 1989 the hydrophone spacing was double that of 1992. These acquisition differences made a direct comparison of the seismic profiles difficult in the time domain, however the use of 3D tomography made it possible to overcome these difficulties (Vesnaver et al., 2003).

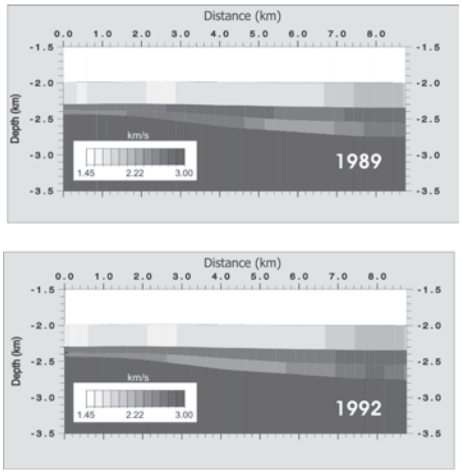

Figure 2. Vertical sections of the 1989 and 1992 3D tomographic models, obtained by a coupled time-lapse inversion.

After independently estimating the velocity models of the two vintages, both the velocities and geometries of the layers were assumed constant in time. They were averaged and used as initial models to improve the velocity fields within the overburden and the reservoir, resulting in two coupled models (see Figure 2). These models have been used as input for a pre-stack depth migration, obtaining the images shown in Figure 3. These sections and the velocity models allow us to verify the changes which occurred within the reservoir during production time.

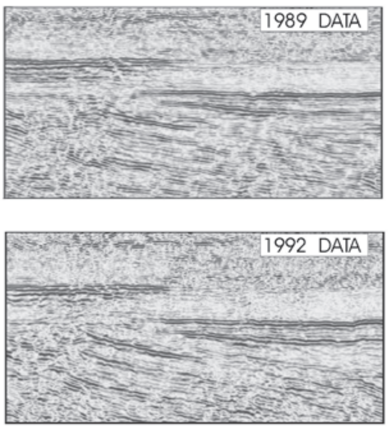

Figure 3. Pre-stack depth-migrated images of the reservoir for the 1989 and 1992 vintages, using coupled velocity models.

3. ROCK PHYSICS

A detailed 3D P and S wave velocity field versus depth is essential to evaluate fluid content, type and saturation, as well as the geopressure conditions. In fact, the seismic response of the subsoil depends on the elastic properties of the subsoil components. In particular, the velocity of seismic waves depends directly upon lithology, saturation and the in-situ conditions.

Generally, rocks in the subsoil are saturated with brine. When other fluids are partially saturating the pore space the elastic properties of the medium may change, resulting in a velocity anomaly relative to the normal trend of a brine saturated rock.

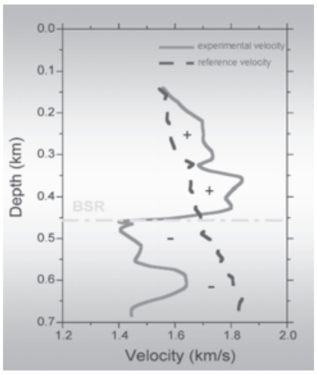

Figure 4. Theoretical velocity of a sedimentary sequence fully brine saturated versus depth (dashed line) and actual velocity (continuous line). Positive velocity anomalies (+) can be related to the presence of gas-hydrate in the pore space and negative anomalies (-) to free gas (Tinivella, 1999).

In Figure 4 the dashed line represents the theoretical velocity versus depth in a brine-saturated sedimentary sequence, while the continuous curve is the actual velocity trend inferred with either tomographic inversion or well-log measurements. Positive velocity anomalies (+) can be related to the presence of gas-hydrate in the pore space and negative anomalies (-) to free gas. Gas-hydrate is an ice-like solid compound where gas molecules, mainly methane, are occluded in a lattice of host water molecules. It forms at low temperature and high pressure conditions and occupies the porous space of the rock, causing a stiffening of the medium and consequently an increasing of the seismic velocity. Layers rich in gas-hydrates may act as cap rocks for trapped free gas underneath. The strong acoustic impedance contrast between high-velocity hydrate-rich and low-velocity free-gas saturated layers causes a strong reflection on seismic sections. Such a signal is called bottom simulating reflector (BSR) and is often used to infer the presence of gas-hydrate within sediments. Above the BSR the pores of the rock are filled with gas hydrate and water, whilst below the BSR the rocks are saturated with free gas and water.

Rock physics is used to establish relationships between rock properties and the observed seismic response. Rock-physics theories can be used to compute theoretical seismic velocities in sediments saturated with fluids or containing gas-hydrates. Rock compositions and fluid saturations can be estimated by comparing the theoretical and observed velocities. There are several theories predicting the elastic properties of composite media. Among them the Biot theory is one of the most commonly used and tested by comparison with laboratory measurements.

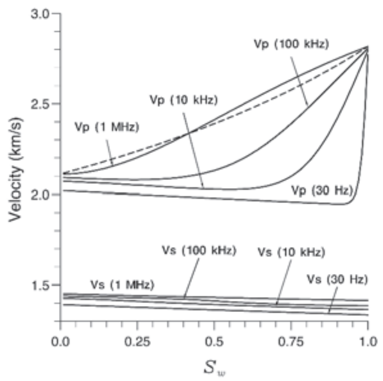

Figure 5. P- and S-wave velocities versus water saturation and different frequencies, using Biot's theory and White's model. The other saturating fluid is free gas and the gas-hydrate fraction is 0.3. Also shown is the P-wave velocity obtained using Hill's equation (dashed line) (Gei and Carcione, 2003).

Figure 5 shows the computed P and S-wave velocities as a function of water saturation (S_w) and frequency of the seismic signal. The matrix is a sandstone and the pore-saturating fluid is a mixture of water and methane whose proportions range from pure gas (S_w=0) to pure water (S_w=1); 30% of the pore space is occupied by gas hydrate. The S-wave velocity is slightly affected by the fluids. The velocity decrease as water saturation increases is due to variations in the density of the composite fluid.

Figure 6 shows the P-wave tomographic velocities of two seismic lines acquired in an area located to the north of the Knipovich Ridge (western Svalbard margin). The dashed line represents the BSR. These velocities have been used to compute the free-gas (methane) saturation and gas-hydrate concentration using a poro-elastic model based on a Biot-type approach (the interaction of the rock frame, gas hydrate and fluid is modeled from first physical principles). By fitting the tomographic velocity fields to theoretical velocities, average hydrate concentrations of 7% and maximum free-gas saturation of 0.4% (uniform saturation) and 9% (patchy saturation), have been obtained. These results are shown in Figure 7.

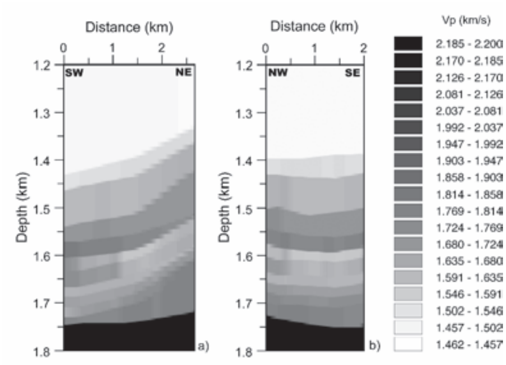

Figure 6. P-wave tomographic velocities of two seismic lines acquired in an area located at the northern side of the Knipovich Ridge (western Svalbard margin). The dashed line represents the BSR (Carcione et al., 2005).

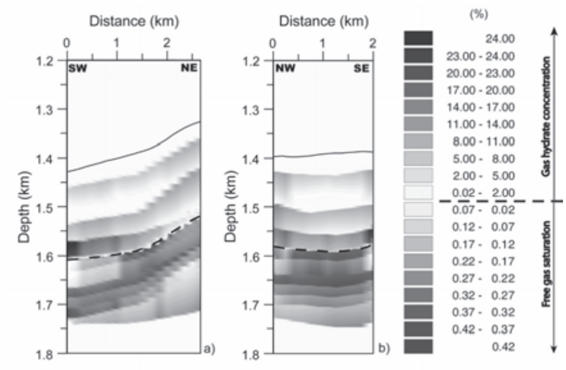

Figure 7. Sections of gas-hydrate concentration (blue color) and free-gas saturation (red color) corresponding to the velocity sections shown in Figure 6. The solid lines indicate the sea bottom and the dashed lines represent the BSR. (Carcione et al., 2005).

Another example of the usefulness and capability of the joint application of tomographic inversion and modeling is the detection of overpressure (Carcione and Tinivella, 2001). A rock is said to be overpressured when its pore pressure (in situ fluid pressure in pores) is significantly greater than the hydrostatic pressure (weight of the overlying pore fluids-mainly brine).

Acoustic and transport properties of rocks generally depend on effective pressure, which is a linear combination of pore and confining pressures. Using the Biot theory of poroelasticity (Biot, 1962; Carcione, 1998) it is possible to calculate the seismic velocities for different combinations of the pore and confining pressures. In particular, Carcione and Tinivella (2001) analysed a site offshore Norway, calibrating a model of the various formations on the basis of well data, tomographic inversion of seismic lines, AVO analysis, and laboratory measurements. The modeling indicated a substantial decrease in velocities with increasing pore-pressure, mainly because of the opening of compliant cracks. The decrease in P-wave velocity is higher for dry rocks than for brine-saturated rocks, while the S-wave velocity is generally higher for the dry case than for the fully brine-saturated case. The presence of gas does not have a major effect on velocities.

4. CONCLUSIONS

Two advanced seismic tools have been presented, namely 3D seismic tomography and poro-elastic modeling. The analysis of the time-lapse North-sea data sets demonstrates the flexibility of tomographic inversion, due to changes in the acquisition geometry and overburden conditions. Analogously, in the case of CO_2 injection, time-lapse tomography can be used to evaluate the subtle changes due to the bubble expansion and possible leakage. The pre-stack depth-migrated sections in depth can be subtracted to evaluate the differences in terms of pressure and saturation. Furthermore, the detection of gas-hydrates and free gas offshore Svalbard has shown that poro-elastic modeling is essential to interpret the velocity changes.

REFERENCES

Arts, R., Chadwick, A., and Eiken, O., 2004, Recent time-lapse seismic data show no indication of leakage at the Sleipner CO2-injection site, *7th Conference on Greenhouse Gas control Technologies*, Vancouver, Canada, 5-9 Sept. 2004.

Bickel, S. H., 1990, Velocity-depth ambiguity of reflection traveltimes, *Geophysics,* **55**:266-276.

Biot, M. A., 1962, Mechanics of deformation and acoustic propagation in porous media. *Journal of Applied Physics* **33**:1482-1498.

Bishop, T., Bube, K., Cutler, R., Langan, R., Love, P., Resinik, J., Shuey, R., Spindler, D., and Wyld, H., 1985, Tomographic determination of velocity and depth in laterally varying media, *Geophysics* 50:903-923.

Böhm, G., Camerlenghi, A., Lodolo, E., and Vesnaver, A., 1995, Tomographic analysis and geological context of a bottom simulating reflector on the South Shetland Margin (Antarctic Peninsula), *Boll. Geof. Teor. Appl*., **37**:3-23.

Carcione, J. M., 1998, Viscoelastic effective rheologies for modelling wave propagation in porous media, *Geophysical Prospecting* **46**:249-270.

Carcione, J. M., and Tinivella, U., 2001, The seismic response to overpressure: a modelling study based on laboratory, well and seismic data., *Geophysical Prospecting* 49:523-539.

Carcione, J. M., Gei, D., Rossi, G. and Madrussani, G., 2005, Estimation of gas hydrate concentraion and free-gas saturation at the Norvegian-Svalbard continental margin. *Geophysical Prospecting*, accepted.

Delprat-Jannaud, F., and Lailly, P., 1992, Ill-posed and well-posed formulations of the reflection traveltime tomography problem, *J. Geophys. Res*., **97(**B13):19827-19844.

Docherty, P., 1992, Solving for the thickness and velocity of the weathering layer using 2-D refraction tomography, *Geophysics* **57**:1307-1318.

Ghaderi, A., and Landrø, M., 2004, Pre-stack estimation of time-lapse seismic velocity changes- an example from the Sleipner CO2-sequestration project, 7th Conference on Greenhouse Gas control Technologies, Vancouver, Canada, 5-9 Sept. 2004.

Gei, D., and Carcione, J. M., 2003, Acoustic properties of sediments saturated with gas hydrate, free gas and water, *Geophysical Prospecting*, **51**:141-157.

Lines, L., 1993, Ambiguity in analysis of velocity and depth, *Geophysics,* **58**:596-597.

Magesan, M., Depagne S., Nixon, K., Regel, B., Opich, J., Rogers, G. and Hudson, T., 2005, Seismic processing for time-lapse study: Genesis field, Gulf of Mexico, *The Leading Edge*, 364-373.

Tieman, H. J., 1994, Investigating the velocity-depth ambiguity of reflection traveltimes, *Geophysics,* 59:1763-1773.

Tinivella, U., 1999, A method for estimating gas hydrate and free gas concentrations in marine sediments, *Boll. Geof. Teor. Appl.,* **40**:19-30.

Vesnaver A. and Böhm G., 2000, Staggered or adapted grids for seismic tomography? *The Leading Edge* **19:**944-950.

Vesnaver, A. L., Accaino, F., Böhm, G., Madrussani, G., Pajchel, J., Rossi, G., and Dal Moro, G., 2003, Time-lapse tomography, *Geophysics* **68:**815-823.